

# Expression profiling identifies the cytoskeletal organizer ezrin and the developmental homeoprotein Six-1 as key metastatic regulators

Yanlin Yu<sup>1,4</sup>, Javed Khan<sup>2,4</sup>, Chand Khanna<sup>2</sup>, Lee Helman<sup>2</sup>, Paul S Meltzer<sup>3</sup> & Glenn Merlino<sup>1</sup>

Patients presenting with metastatic rhabdomyosarcoma (RMS), the most common soft-tissue sarcoma in children, have a very poor clinical prognosis. This is due, in large part, to our rudimentary knowledge of the molecular events that dictate metastatic potential. We used cDNA microarray analysis of RMS cell lines, derived from Ink4a/Arf-deficient mice transgenic for hepatocyte growth factor/scatter factor (HGF/SF), to identify a set of genes whose expression was significantly different between highly and poorly metastatic cells. Subsequent *in vivo* functional studies revealed that the actin filament–plasma membrane linker ezrin (encoded by *Vil2*) and the homeodomain-containing transcription factor Six-1 (*sine oculis*-related homeobox-1 homolog) had essential roles in determining the metastatic fate of RMS cells. *VIL2* and *SIX1* expression was enhanced in human RMS tissue, significantly correlating with clinical stage. The identification of ezrin and Six-1 as critical regulators of metastasis in RMS provides new mechanistic and therapeutic insights into this pediatric cancer.

RMS, a skeletal muscle cancer, accounts for 5–10% of all pediatric neoplasms and >50% of pediatric soft-tissue sarcomas<sup>1</sup>. Despite recent improvements in long-term survival rates, about one third of RMS patients continue to experience relapses, and the majority of these patients die from disseminated metastatic disease<sup>2,3</sup>, illustrating the need for new therapeutic strategies. Metastasis is a complex and multistage process involving local invasion, intravasation, successful transit through the bloodstream, extravasation, and eventual proliferation and survival within a favorable target organ. Although individual candidate genes have been implicated in the metastatic process, few such discoveries have led to substantial clinical improvement. Advances in microarray-based expression profiling have provided technology robust enough to enable simultaneous analysis of the expression of large groups and combinations of genes. This technology has recently been brought to bear on the challenge of tumor progression and metastasis<sup>4–6</sup>.

Microarray-based expression profiling has been most commonly used to compare and contrast heterogeneous groups of human tumors. But such analyses are more difficult in RMS and other relatively rare tumors for which it is difficult to procure tissue samples of sufficient numbers to ensure statistical significance. The availability of an authentic mouse model that accurately reflects human disease would offer the possibility of analyzing larger numbers of homogeneous tumor samples, thus increasing the likelihood of identifying crucial metastasis genes and pathways. We recently reported the development of a transgenic mouse, overexpressing the c-Met ligand HGF/SF and deficient in

Ink4a/Arf, in which skeletal muscle tumors reminiscent of those in embryonic RMS arise with very high penetrance and short latency<sup>7</sup>. All HGF/SF-transgenic, Ink4a/Arf-deficient mice succumb to multifocal, highly invasive RMS tumors by ~4 months of age. Here we used this transgenic model system to establish a panel of highly and poorly metastatic RMS cell lines, which we subjected to microarray-based expression profiling to generate hypotheses as to which genes contribute to the metastatic process. We then validated several candidate genes using a variety of functional studies.

## Establishment of highly and poorly metastatic RMS cell lines

Early-passage RMS cell lines were derived predominantly from RMS tumors arising in a variety of primary sites in HGF/SF-transgenic, Ink4a/Arf-deficient mice (Table 1). The metastatic potential of each of 19 of these cell lines was assessed *in vivo* by tail vein injection and orthotopic transplantation with spontaneous metastases. There was good general agreement between the results obtained using these two techniques. Nine cell lines were designated as highly metastatic to the lung, while ten others were deemed to be poorly metastatic (Table 1). Metastasis was noted in other organs, including kidney, heart, liver and skin. The highly and poorly metastatic cell lines could not be distinguished *in vitro* by morphology or growth characteristics (data not shown). An assessment of expression and activity of obvious candidate pathway members, such as c-Met, AKT and MAPK, revealed no consistent differences (Supplementary Fig. 1 online). We therefore analyzed global gene expression patterns using a cDNA microarray approach.

<sup>1</sup>Laboratory of Molecular Biology and <sup>2</sup>Pediatric Oncology Branch, National Cancer Institute, National Institutes of Health, Bethesda, Maryland 20892, USA. <sup>3</sup>Cancer Genetics Branch, National Human Genome Research Institute, National Institutes of Health, Bethesda, Maryland 20892, USA. <sup>4</sup>These authors contributed equally to this work. Correspondence should be addressed to G.M. (gmerlino@helix.nih.gov).

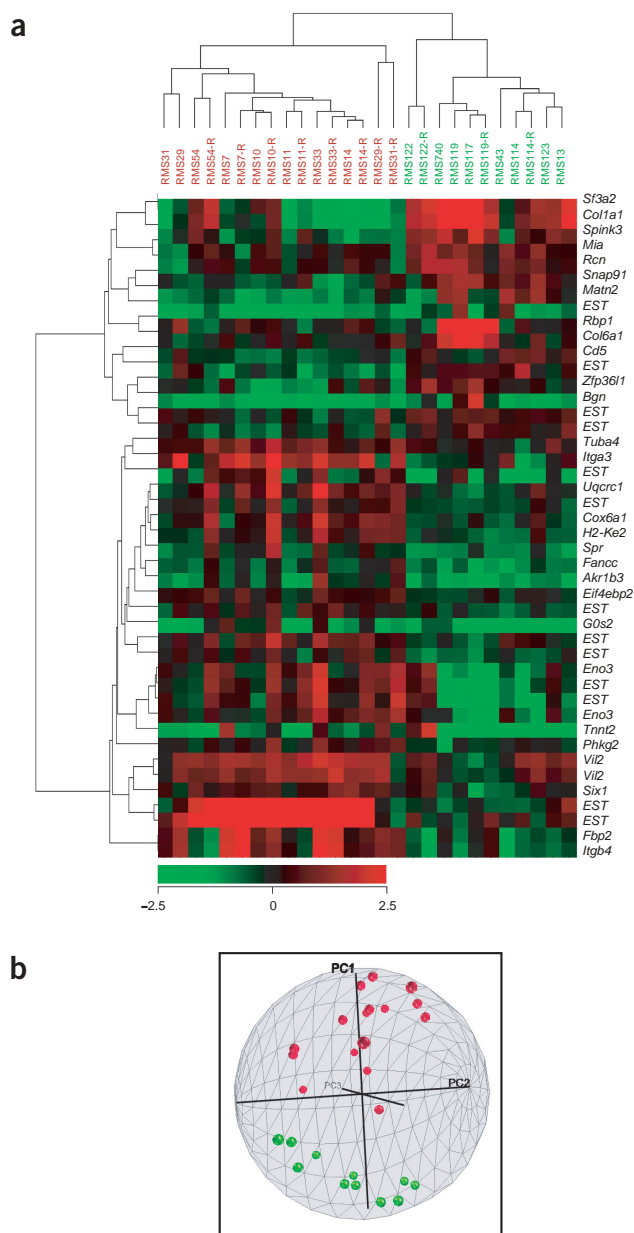


**Figure 1** cDNA microarray analysis of highly and poorly metastatic RMS cell lines. **(a)** Hierarchical clustering using Pearson correlation distance and average linkage of cell lines and genes. Each row represents 1 of 44 cDNA clones; each column represents a separate cell line experiment. –R indicates reverse-dye experiment. Pseudocolored representation of  $\log_2$  ratio is shown. High and low expression relative to control are shown in red and green, respectively. Genes appear twice because duplicate clones were present on the array. **(b)** Three-dimensional plot of principal component (PC) analysis of 44 genes. Shown is one projection of the first three principal components. High and low metastatic lines are shown as red and green spheres, respectively.

dye-reversed experiments), we used random permutation-weighted gene analysis to identify the most significant differentially expressed genes between the highly and poorly metastatic lines, and used these to classify the phenotypes of the samples<sup>9</sup>. The highly and poorly metastatic RMS cell lines clustered into two separate classes (Fig. 1a,b).

Western and northern blots were used to verify that the microarray data was an accurate representation of the gene expression patterns in the RMS cells. We focused on a representative set of genes that was overexpressed in the highly metastatic RMS cells. As predicted, ezrin, enolase-3 and  $\alpha_3$  integrin protein were all significantly overexpressed in highly metastatic, compared with poorly metastatic, RMS cell lines ( $P = 0.006$ ,  $0.001$  and  $0.0001$ , respectively; Fig. 2a). Northern blot hybridization was used to show that *Six1* gene expression was also significantly increased in highly metastatic RMS cells ( $P < 0.0001$ ; Fig. 2b). These results indicate that the microarray analysis was an accurate representation of gene expression in these RMS cell lines. *VIL2* and *SIX1* expression was also assessed in stage 1, 2 and 4 human RMS tissues. Notably, *VIL2* and *SIX1* were both overexpressed in human RMS, with expression levels significantly correlating with progression ( $P = 0.016$  and  $0.018$ , respectively; Fig. 3a,b).

### Ezrin as a regulator of metastasis in RMS cells

A metastatic role for ezrin, a member of the ezrin/radixin/moesin (ERM) protein family, was experimentally assessed by transfection of a *VIL2* expression vector into the poorly metastatic, low-ezrin cell lines RMS119 and RMS772. We selected stable cell lines expressing high levels of ezrin (Fig. 4a), and tested them for their ability to metastasize when introduced into nude mice by tail vein injection. Expression of wild-type ezrin significantly stimulated pulmonary metastasis in both RMS119 and RMS772, by a factor of greater than tenfold ( $P = 0.0001$  and  $P = 0.01$ , respectively; Fig. 4b).

To further show the role of ezrin in RMS cell metastasis, we disrupted ezrin activity in a highly metastatic RMS cell line using two approaches. In one set of experiments, we introduced the ezrin mutant T567A, which lacks the critical threonine phosphorylation site and is believed to act as an ezrin dominant-negative agent<sup>10–12</sup>, into the highly metastatic cell line RMS14, which overexpresses ezrin. Stable clones expressing high levels of T567A were then selected (Fig. 4a). The phenotypic consequences of T567A expression were determined using assays for branching morphogenesis and vasculogenic mimicry, which are associated with a highly invasive, metastatic phenotype<sup>13,14</sup>. RMS14 cells, normally adept at forming cellular processes and tubules, remained as cysts and did not exhibit branching morphogenesis when expressing T567A at levels that were equivalent to those of endogenous ezrin (Fig. 4c), indicating that this mutant can effectively block ezrin function in RMS cells. Similarly, T567A expression inhibited the development of vessel-like networks in RMS14 cells (Fig. 4d).

### Expression profiling of metastatic determinants in RMS

Expression profiling was done using total RNA from eight highly and nine poorly metastatic RMS cell lines, and microarrays enriched for clones representing mouse developmental genes<sup>8</sup>. In all experiments, RNA from the nonmetastatic cell line RMS772 was used as the common reference. Forty-four cDNAs, of the 3,949 examined, were differentially expressed to a significant degree ( $P < 0.001$ ; Fig. 1). Twenty-eight genes were overexpressed in highly metastatic cells, including those encoding the adhesion molecules ezrin (encoded by *Vil2*),  $\alpha_3$  integrin and  $\beta_4$  integrin, the homeodomain-containing transcription factor Six-1, and the muscle proteins enolase-3 and tropinin T2. In contrast, expression of 16 gene products, including retinol binding protein, procollagen type IV- $\alpha_1$ , *Zfp3611*, biglycan and matrilin, were downregulated in highly metastatic RMS cells. The expression patterns varied, but the majority of the outlying genes were common between replicate experiments. Using this list of genes and the data from 27 experiments (17 samples, several repeated in

The T567A-expressing RMS14 cells were next introduced into nude mice by tail vein injection to assess the consequences of ezrin disruption on metastasis. The presence of the T567A inhibited pulmonary metastasis by more than tenfold (Fig. 4b). In a second, related set of experiments, RMS14 cells were stably transfected with an ezrin short hairpin RNA (shRNA) expression vector. The shRNA reduced the expression of ezrin in RMS14 cells by 2.9-fold (Fig. 4a). When these cells were injected into nude mice, expression of the shRNA significantly inhibited pulmonary metastasis ( $P = 0.04$ ; Fig. 4b). Taken together, these data indicate that ezrin is an important determinant of metastatic potential in RMS cells, and may be required for efficient metastasis.

Studies have shown that activation of ERM proteins is linked to the Rho signaling pathways<sup>15,16</sup>. Upon examination of Rho GTPase activity in representative RMS cell lines, we generated data suggesting a general correlation between ezrin expression and Rho activity in RMS cells (data not shown). Overexpression of sense ezrin enhanced Rho activity in two poorly metastatic RMS cell lines, whereas expression of the T567A ezrin mutant diminished Rho activity in the highly metastatic RMS14 cells (Fig. 4e). Forced expression of a dominant-negative mutant RhoA also significantly inhibited metastatic potential in RMS14 cells ( $P < 0.05$ ; Fig. 4f), albeit not as markedly as did the T567A ezrin mutant (Fig. 4b). These data are consistent with the

**Table 1** Metastatic behavior of RMS cell lines

Cell line	Genotype <sup>a</sup>		Primary site	Gross pulmonary metastasis	
	Ink4a/Arf	HGF/SF		Tail vein injection	Orthotopic transplant <sup>b</sup>
RMS2	Null	+	Subcutaneous	Extensive	Extensive
RMS7	Het	+	Spine	Extensive	—
RMS10	Het	+	Rib	Extensive	Extensive
RMS11	Null	+	Abdominal	Extensive	Extensive
RMS14	Null	+	Hip	Moderate	Extensive
RMS29	WT	+	Cervical	Extensive	—
RMS31	Null	+	Leg	Extensive	Extensive
RMS33	Null	+	Leg	Extensive	—
RMS54	Null	+	Sternum	Extensive	—
RMS13	Null	+	Rib	None	Light
RMS32	Null	+	Subcutaneous	None	Light
RMS43	Null	+	Subcutaneous	None	Extensive
RMS114	Null	+	Leg	None	—
RMS117	Null	—	Ear	None	—
RMS119	Null	+	Subcutaneous	None	—
RMS122	Null	+	Rib	None	—
RMS123	Null	+	Subcutaneous	None	—
RMS740	Null	+	Diaphragm	None	Light
RMS772	Null	+	Subcutaneous	None	None

Metastatic tumor spread was classified as extensive, moderate, light or none based on gross observation of pulmonary lesions at necropsy. Samples RMS2 and RMS32 failed quality control and were excluded from subsequent array analysis. <sup>a</sup>Het, heterozygous; WT, wild type; + or —, presence or absence, respectively, of MT-HGF/SF transgene.

<sup>b</sup>Intramuscular orthotopic transplantation was done as described<sup>4,45</sup>; —, not done.

notion that ezrin influences metastatic potential, at least in part, through the Rho family of proteins.

### Six-1 as a regulator of metastasis in RMS cells

To examine the role of expression of the developmental transcription factor Six-1 in metastasis, a mouse *Six1* expression vector was stably introduced into two poorly metastatic RMS cell lines with low Six-1 expression (RMS119 and RMS772). Transfected RMS119 and RMS772 cells with high Six-1 expression (Fig. 5a) were introduced by tail-vein injection into nude mice, where they produced significantly elevated numbers of pulmonary metastases compared with parental lines ( $P < 0.005$  and  $0.01$ , respectively; Fig. 5b). In contrast, forced Six-1 expression had no substantial effect on pulmonary metastasis of the highly metastatic line RMS14, which already expressed relatively high levels of Six-1 (Fig. 5a,b). Conversely, stable expression of *Six1*-specific shRNA reduced Six-1 expression by 3.6-fold and inhibited pulmonary metastasis of highly metastatic RMS14 cells by a factor of seven (Fig. 5a,b). These data show that the status of Six-1 expression can have a profound effect on metastasis. Consistent with a previous report on the effect of Six-1 on the cell cycle<sup>17,18</sup>, RMS cells overexpressing Six-1 showed enhanced *in vitro* proliferation, as well as increased cellular invasiveness (Fig. 5c). Notably, forced Six-1 expression

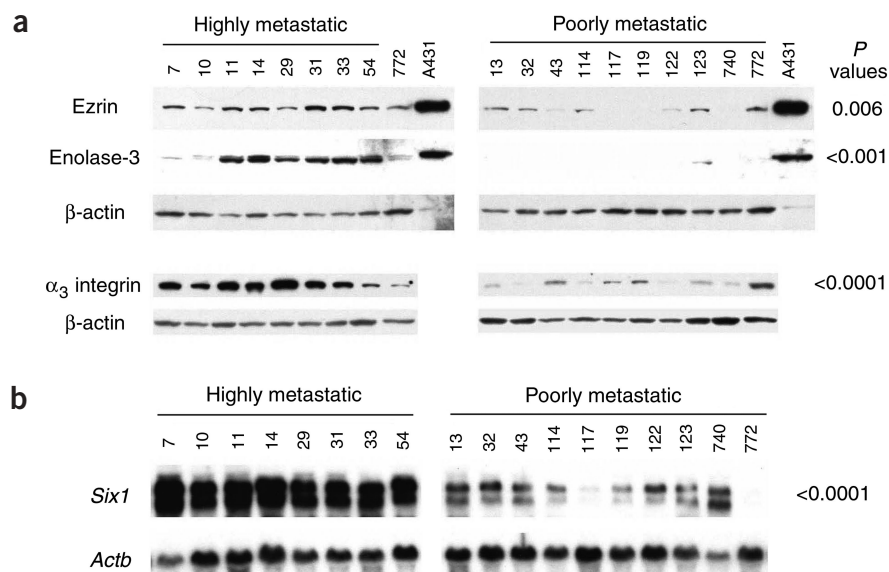


**Figure 2** Validation of genes identified by cDNA microarray analysis as significantly overexpressed in highly and poorly metastatic cells. (a) Western blot analysis of ezrin, enolase-3 and  $\alpha_3$  integrin expression. (b) Northern blot analysis of *Six1* expression. Numbers at the top of each panel refer to RMS cell lines listed in Table 1.  $\beta$ -actin was used as a control. Significance (by paired Student *t*-test) of differential expression between highly and poorly metastatic groups is shown at right.

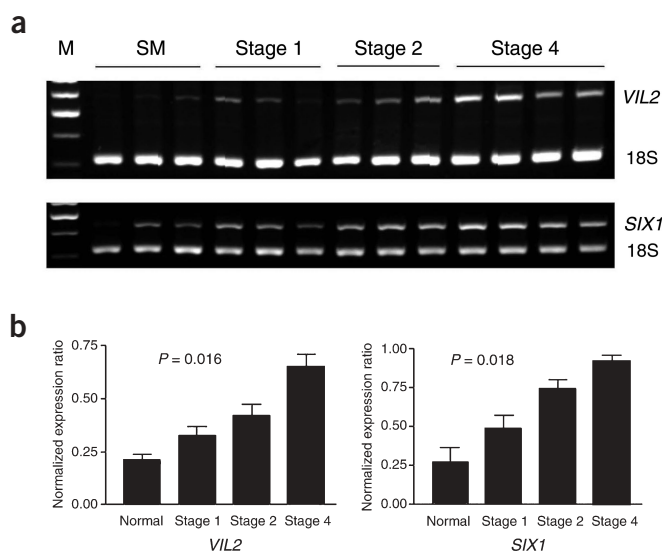


**Figure 3** Analysis of expression of *VIL2* and *SIX1* in staged human RMS tissue. **(a)** Quantitative RT-PCR analysis of expression of human genes encoding ezrin and Six-1 in representative stage 1, 2 and 4 RMS neoplasms, compared with normal human skeletal muscle (SM). Expression of 18S rRNA (18S) was used as internal control. Northern blot analysis confirmed these expression patterns (data not shown). M, molecular weight markers. **(b)** Relative expression of human *VIL2* and *SIX1* in staged human RMS tumors compared with normal skeletal muscle. Bars indicate s.e.m. *P* values were assigned using Kruskal-Wallis one-way nonparametric ANOVA.

also induced upregulation of ezrin in two poorly metastatic RMS cell lines, suggesting that *Vil2* lies downstream of *Six1* (Fig. 5d).

## DISCUSSION

Tumor progression to a fully malignant, metastatic phenotype is a highly complex process involving alterations in the expression of a multitude of genes. The advent of microarray technology, in which the expression of tens of thousands of genes can be assessed simultaneously, has greatly facilitated the dissection of this process<sup>4-6,9,19</sup>. Here we describe the use of cDNA microarray analysis to identify a set of genes whose enhanced expression is associated with metastasis in cell lines established from a recently developed mouse model of human RMS<sup>7</sup>. We experimentally demonstrate *in vivo*, for the first time, the functional metastatic role of two of these genes, *Vil2* and *Six1*.

Ezrin is a member of the ERM family, which shares the common membrane-binding N-terminal FERM domain with band-4.1 family members<sup>15,16</sup>. Ezrin provides a functional link between the plasma membrane and the cortical actin cytoskeleton of the cell, and participates in crucial signal transduction pathways. ERM members undergo phosphorylation at a C-terminal threonine through kinases such as Rho kinase<sup>10,20</sup>, and at N-terminal tyrosines through receptor tyrosine kinases such as the epidermal growth factor receptor and c-MET<sup>21,22</sup>, promoting cytoskeletal reorganization and subsequent morphogenetic alterations. Ezrin has been implicated in the metastatic spread of osteosarcoma and mammary and pancreatic adenocarcinomas<sup>4,12,23</sup>. Here we reported that ezrin expression significantly correlates with metastasis in our mouse RMS model system. We also demonstrated experimentally that forced ezrin expression induces a highly metastatic state in poorly metastatic RMS cell lines.

Ezrin resides at the nexus of multiple pathways regulating cellular behaviors that can influence metastatic potential, including cell survival, motility, invasion and adherence<sup>12,15,16,24</sup>. Analysis of the phenotype of RMS14 cells transfected with the dominant-negative ezrin mutant T567A strongly supports the association of ezrin expression with aggressive malignancy. Our data also suggest that the prometastatic activity of ezrin is mediated, at least in part, through Rho. The Rho family of small G proteins regulates a variety

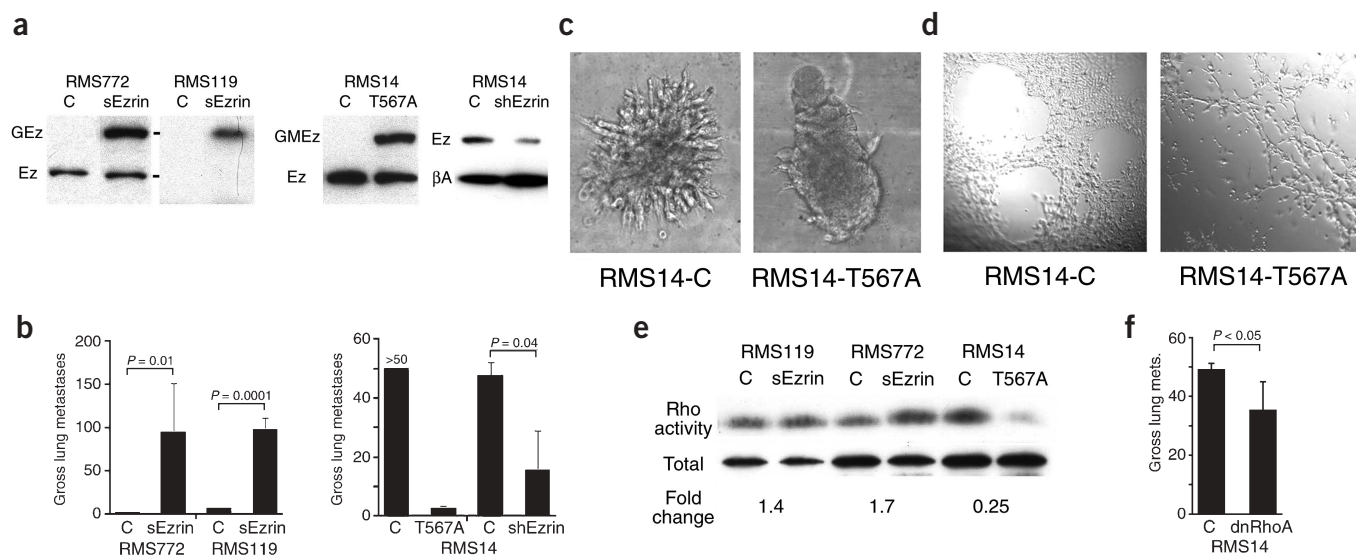


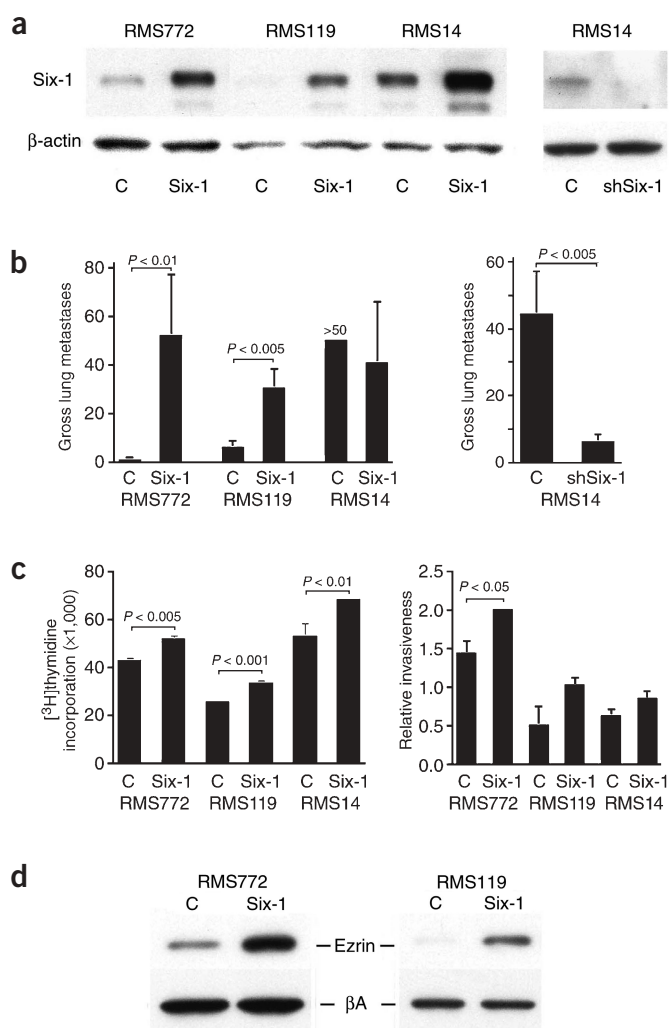
**Figure 4** Phenotypic consequences of altered Ezrin function. **(a)** Western blot analysis of stable RMS cell lines transfected with plasmids expressing sense *Vil2* (sEzrin), T567A ezrin mutant, or ezrin-targeted shRNA (shEzrin). RMS772 and RMS119 are poorly metastatic; RMS14 is highly metastatic. sEzrin and T567A mutant were expressed as GFP fusion proteins (GEz and GMEz, respectively). Ez, ezrin; βA, β-actin control. **(b)** Gross pulmonary metastases from transfected cells. Bars indicate s.e.m.; >50 indicates too numerous to count. **(c, d)** Light microscopy showing that T567A inhibits branching morphogenesis **(c)** and formation of vessel-like networks **(d)** C, vector control. Magnification, approximately  $\times 100$ . **(e)** Alterations in functional ezrin levels induce corresponding changes in Rho activity. **(f)** Effect of dominant-negative RhoA (dnRhoA) on pulmonary metastasis of RMS14 cells.

**Figure 5** Phenotypic consequences of altered Six-1 expression. **(a)** Western blot analysis of representative RMS cell lines stably transfected with constructs expressing either sense, full-length Six-1 or a Six-1-targeted shRNA (shSix-1). RMS772 and RMS119 are poorly metastatic; RMS14 is highly metastatic. C, vector control. **(b)** Gross pulmonary metastases from transfected cell lines. **(c)** Forced expression of Six-1 stimulated cellular proliferation (left) and invasiveness (right) *in vitro*. Bars indicate s.e.m. (not visible if low); >50 indicates too numerous to count. **(d)** Western blot analysis of ezrin expression in poorly metastatic RMS cells transfected with a sense full-length Six-1 expression vector.  $\beta$ A,  $\beta$ -actin control.

of cellular functions through actin cytoskeletal reorganization, is deregulated in many tumor types, and is capable of inducing a variety of cellular behaviors associated with tumor progression<sup>25,26</sup>. ERM proteins such as ezrin function both upstream and downstream of Rho, forming an amplification feedback system<sup>15,16</sup>. For example, ERM proteins can bind to the Rho negative regulator RhoGDI, thereby releasing inactive Rho and facilitating its activation<sup>27</sup>. ERM interaction with hamartin, the protein product of the tumor suppressor gene *TSC1*, activates Rho and promotes focal adhesion formation<sup>28</sup>. In this report, we showed that using T567A to compromise ezrin function in highly metastatic RMS14 cells inhibits both Rho activity and metastatic potential, an effect also achieved through expression of dominant-negative RhoA. Notably, Rho proteins are also activated through interactions with integrins<sup>29,30</sup>, several of which are characteristically upregulated in our metastatic RMS cells.

In contrast to the cytoskeletal organizer ezrin, Six-1 is a homeo-domain-containing transcription factor, a vertebrate homolog of the *Drosophila* gene *sine oculis* gene that is implicated in the development of muscle, eye and brain<sup>31</sup>. In cultured human cells, Six-1 expression is normally upregulated during S-phase entry, and forced Six-1 expression attenuates a DNA damage-induced G2 cell cycle checkpoint<sup>17</sup>. Six-1 is also phosphorylated by casein kinase II, which may regulate its cell cycle control function<sup>18</sup>. In support of these studies, we found that RMS cells overexpressing Six-1 showed enhanced proliferative capacity *in vitro*. However, the enhancing effect of Six-1 expression on *in vitro* invasiveness suggests a more complex role in cellular behavior. In fact, Six-1 is expressed in migrating limb precursor cells, acts as part of a regulatory network along with *Eya-2*, *Dach-2* and *Pax-3* (refs. 32,33), and is required for primary myogenesis<sup>34</sup>. Six-1 was itself induced in NIH3T3 cells by forced expression of the alveolar RMS-derived fusion oncogene *Pax3-Foxo1* (ref. 8). Six-1 also activates myogenin expression by interacting with MEF-3 binding sites, which have been implicated in the regulation of other skeletal muscle-related genes<sup>35</sup>. Another potential transcriptional target of the Six-1/*Eya-2*/*Dach-2*/*Pax-3* regulatory network is *Lbx1h*, a homeobox gene required for migration of muscle precursor cells<sup>36</sup>. This raises the possibility that overexpression of Six-1 may induce metastatic spread by subverting the normal role of *Lbx1h* in regulating myoblast migration.

The sharp behavioral separation observed between our highly and poorly metastatic cell lines constitutes genetic evidence supporting the notion that a relatively small number of crucial regulatory factors may dictate metastatic potential. The existence of such key metastasis regulators could account, in part, for the detection of common metastatic signatures by microarray analysis of human tumors<sup>5,6</sup>, as well as the coordinated upregulation of prometastatic genes, such as *Vil2* and certain integrins, in our RMS model. Six-1, a transcription factor that helps control development-related cellular behavior, is a possible candidate for such a metastasis regulator. In fact, ezrin



expression was enhanced in poorly metastatic RMS cell lines in which Six-1 expression was experimentally elevated. Six-1 was also reported to be upregulated in primary and metastatic breast cancer<sup>17</sup>. Thus, this transcription factor may influence expression of a battery of genes associated with cell proliferation, survival, motility and/or invasiveness.

Here we demonstrate the power of applying microarray-based genomic analysis in combination with genetically engineered mouse models to the study of metastasis. The successful identification and functional confirmation of ezrin and Six-1 as important metastatic regulators offers new mechanistic insights into RMS. The HGF/SF-transgenic, *Ink4a/Arf*-deficient mouse model can also serve as a potential preclinical model system. Both *Vil2* and *Six1* are members of a panel of genes whose predictive value with respect to metastatic potential can now be validated prospectively using our mouse model, as well as retrospectively in human RMS samples. In addition, cell lines with highly metastatic and poorly metastatic profiles can be used in syngeneic transplantation assays to test the efficacy of promising rational antimetastatic agents derived from expression profiling data. The degree to which ezrin influences metastatic potential in this model system raises the possibility that it could be used as a molecular target in antimetastasis therapy. A successful outcome from studies such as these should brighten the therapeutic prospects for advanced RMS cases.

## METHODS

**Establishment of RMS cell lines.** Highly and poorly metastatic cell lines were derived from RMS arising in HGF/SF-transgenic, Ink4a/Arf-deficient mice, generated on an FVB/N-C57BL/6 background as described<sup>7</sup>. RMS cells were maintained in RPMI1640 medium with 10% FBS (Gibco). All microarray experiments were done with cells of relatively early passages (3–15). The full-length human *VIL2* construct was a gift from R. Lamb (University College London). Wild-type and T567A *VIL2* were subcloned into pEGFPN1 expression vectors. Mouse *Six1* expression plasmid was a gift from P. Maire (Institut Cochin-INSERM 567). Dominant-negative RhoA (T19N) expression vector was purchased from Upstate Cell Signaling Solutions (catalog no. 21-196). Overexpression vectors were transfected using Lipofectamine Plus (Invitrogen). At least two independent stable lines were tested for all constructs. To establish stable cell lines expressing shRNA, double-stranded DNA directed against nucleotides 174–194 and 100–120 of the mouse *Vil2* (GenBank accession no. NM\_009510) and *Six1* (GenBank accession no. X80339) coding regions, respectively, were synthesized and cloned into the pSUPER vector (OligoEngine; ref. 37), transfected into RMS cells and selected with puromycin.

**RNA extraction and analysis.** Total RNA was extracted using TRIzol (Life Technologies), quantified and used for microarray, northern blot and RT-PCR experiments. Use of human tissue samples was approved by the Institutional Review Board of the National Cancer Institute. The Cooperative Human Tissue Network supplied human tissue samples. Appropriate informed consent was obtained before tissue acquisition.

**cDNA microarray analysis.** The mouse array was composed of 3,949 detector elements as described<sup>8</sup>. Of these, 315 were unclustered ESTs, 630 were clustered ESTs and 3,004 were clustered, named genes. There was substantial redundancy in the named gene portion of the set; only 2,221 unique clusters were represented. PCR products from clones (Research Genetics) were prepared and printed onto glass slides as described<sup>38</sup>. Fluorescent Cy3- or Cy5-labeled cDNA (Amersham Pharmacia Biotech) was synthesized from 100–200 µg total RNA, using oligo dT-primed polymerization with SuperScript II reverse transcriptase (Life Technologies)<sup>38</sup>. Each array experiment used the same reference RNA from RMS772 cells; reverse array experiments were done with same RNA. Fluorescence intensities at the immobilized targets were measured using a GenPix scanner; scanned images were analyzed using DeArray software<sup>39</sup>. Our microarray data can be found at [http://home.ccr.cancer.gov/oncology/oncogenomics/Yu\\_et\\_al\\_data.htm](http://home.ccr.cancer.gov/oncology/oncogenomics/Yu_et_al_data.htm).

**Procedure for gene selection.** To distinguish between highly and poorly metastatic groups, all experiments, including duplicates, were counted as single experiments, resulting in a comparison of 16 experiments using highly metastatic lines (eight unique, eight duplicates) with 11 using poorly metastatic lines (eight unique, three duplicates). Genes were filtered to include only those genes whose average quality was >0.5 across all experiments, according to published algorithms<sup>40</sup>. We calculated a discriminative weight ( $\omega$ ) for each gene using the equation  $\omega = d_B / (k_1 d\omega_1 + k_2 d\omega_2 + \delta)$ , where  $d_B$  is the center-to-center distance (between-cluster Euclidean distance),  $d_\omega$  is the average Euclidean distance among all sample pairs, and the total of  $t_1$  and  $t_2$  sample pairs for clusters 1 (high) and 2 (low), respectively, and  $k_1 = t_1 / (t_1 + t_2)$ , and  $k_2 = t_2 / (t_1 + t_2)$  (ref. 9).  $\delta$  is a small constant (0.1) to prevent a zero denominator. Genes were ranked on the basis of  $\omega$ . We randomized the labels of samples 1,000 times, calculated  $P$  and  $\alpha$  as described<sup>41</sup> and selected genes whose weight was >1.4 ( $P < 0.001$ ,  $\alpha < 0.001$ ), resulting in the survival of 44 elements.

**Western blot analysis.** Immunoblots were performed on lysates generated from cultured cells and tissues solubilized in RIPA buffer<sup>42</sup>. We used antibodies to ezrin (Upstate Biotechnology); Six-1, enolase-3,  $\beta_4$  integrin,  $\beta$ -actin, RhoA, HGF and c-Met (Santa Cruz Biotechnology);  $\alpha_3$  integrin (Chemicon International); enolase/ENO-3 (BD Transduction Laboratories); phosphorylated Akt(Ser473)4E2 (monoclonal), phosphorylated Akt(Thr308) (polyclonal), Akt (polyclonal), p42/44 and phosphorylated p42/44 (Cell Signaling Technology); phosphotyrosine (PY20; Transduction Laboratories); and live color (Clontech). Rho activity was quantified using the Rho activation assay kit (Upstate Cell Signaling Solutions), according to the manufacturer's instructions.

**In vitro cellular behavior assays.** Proliferation rates were determined by [<sup>3</sup>H]thymidine incorporation as described<sup>43</sup>. An *in vitro* three-dimensional cell culture assay was used to assess branching morphogenesis<sup>44</sup> of  $3 \times 10^3$  cells in ECMatrix gel (Chemicon). Formation of patterned vessel-like networks (vasculogenic mimicry) was assessed using  $10^4$  RMS cells cultured on ECMatrix gel, monitored under an inverted light microscope at magnifications of  $\times 20$  to  $\times 100$  (ref. 13). The paired Student *t*-test was used for statistical analysis.

**Experimental and spontaneous metastasis assays.** For tail vein injection assays,  $10^5$  or  $10^6$  cells were intravenously injected into 5- to 6-week-old male athymic nude mice<sup>42</sup>. Tumor number was obtained by visual inspection of tissues in mice killed 21 d after transplantation. For spontaneous metastasis, orthotopic transplantation of  $2 \times 10^6$  viable cells to the left hind gastrocnemius muscle was done as described<sup>4,45</sup>. Mice were evaluated three times a week. Tumor-bearing limbs were amputated at a tumor size of 1.2 cm. Complete necropsy allowed the definition of distant metastases in all mice. All mouse work was done with the approval of the Animal Care and Use Committee of the National Cancer Institute.

*Note: Supplementary information is available on the Nature Medicine website.*

## ACKNOWLEDGMENTS

The authors thank P. Maire for the full-length mouse *Six1* expression plasmid, R. Lamb for the full-length human *VIL2* construct, and H. Takayama and R. Herring for assistance with the RMS cell lines. This work was supported in part by the Cooperative Human Tissue Network, which is funded by the National Cancer Institute.

## COMPETING INTERESTS STATEMENT

The authors declare that they have no competing financial interests.

Received 9 September; accepted 4 November 2003

Published online at <http://www.nature.com/naturemedicine/>

- Merlino, G. & Helman, L.J. Rhabdomyosarcoma—working out the pathways. *Oncogene* **18**, 5340–5348 (1999).
- Dagher, R. & Helman, L. Rhabdomyosarcoma: an overview. *Oncologist* **4**, 34–44 (1999).
- Ruymann, F.B. & Grovas, A.C. Progress in the diagnosis and treatment of rhabdomyosarcoma and related soft tissue sarcomas. *Cancer Invest.* **18**, 223–241 (2000).
- Khanna, C. *et al.* Metastasis-associated differences in gene expression in a murine model of osteosarcoma. *Cancer Res.* **61**, 3750–3759 (2001).
- Ramaswamy, S., Ross, K.N., Lander, E.S. & Golub, T.R. A molecular signature of metastasis in primary solid tumors. *Nat. Genet.* **33**, 49–54 (2003).
- Ye, Q.H. *et al.* Predicting hepatitis B virus-positive metastatic hepatocellular carcinomas using gene expression profiling and supervised machine learning. *Nat. Med.* **9**, 416–423 (2003).
- Sharp, R. *et al.* Synergism between INK4a/ARF inactivation and aberrant HGF/SF signaling in rhabdomyosarcomagenesis. *Nat. Med.* **8**, 1276–1280 (2002).
- Khan, J. *et al.* cDNA microarrays detect activation of a myogenic transcription program by the PAX3-FKHR fusion oncogene. *Proc. Natl. Acad. Sci. USA* **96**, 13264–13269 (1999).
- Bittner, M. *et al.* Molecular classification of cutaneous malignant melanoma by gene expression profiling. *Nature* **406**, 536–540 (2000).
- Tran Quang, C., Gautreau, A., Arpin, M. & Treisman, R. Ezrin function is required for ROCK-mediated fibroblast transformation by the net and dbl oncogenes. *EMBO J.* **19**, 4565–4576 (2000).
- Ng, T. *et al.* Ezrin is a downstream effector of trafficking PKC-integrin complexes involved in the control of cell motility. *EMBO J.* **20**, 2723–2741 (2001).
- Khanna, C. *et al.* Ezrin, a membrane-cytoskeleton linker, is necessary for osteosarcoma metastasis. *Nat. Med.* (in the press).
- Maniotis, A.J. *et al.* Vascular channel formation by human melanoma cells *in vivo* and *in vitro*: vasculogenic mimicry. *Am. J. Pathol.* **155**, 739–752 (1999).
- Zhang, Y.W. & Vande Woude, G.F. HGF/SF-met signaling in the control of branching morphogenesis and invasion. *J. Cell. Biochem.* **88**, 408–417 (2003).
- Louvet-Vallee, S. ERM proteins: from cellular architecture to cell signaling. *Biol. Cell* **92**, 305–316 (2000).
- Bretscher, A., Edwards, K. & Fehon, R.G. ERM proteins and merlin: integrators at the cell cortex. *Nat. Rev. Mol. Cell Biol.* **3**, 586–599 (2002).
- Ford, H.L., Kabingu, E.N., Bump, E.A., Mutter, G.L. & Pardee, A.B. Abrogation of the G2 cell cycle checkpoint associated with overexpression of HSIX1: a possible mechanism of breast carcinogenesis. *Proc. Natl. Acad. Sci. USA* **95**, 12608–12613 (1998).

18. Ford, H.L. *et al.* Cell cycle-regulated phosphorylation of the human SIX1 homeodomain protein. *J. Biol. Chem.* **275**, 22245–22254 (2000).
19. Clark, E.A., Golub, T.R., Lander, E.S. & Hynes, R.O. Genomic analysis of metastasis reveals an essential role for RhoC. *Nature* **406**, 532–535 (2000).
20. Matsui, T. *et al.* Rho-kinase phosphorylates COOH-terminal threonines of ezrin/radixin/moesin (ERM) proteins and regulates their head-to-tail association. *J. Cell Biol.* **140**, 647–657 (1998).
21. Krieg, J. & Hunter, T. Identification of the two major epidermal growth factor-induced tyrosine phosphorylation sites in the microvillar core protein ezrin. *J. Biol. Chem.* **267**, 19258–19265 (1992).
22. Crepaldi, T., Gautreau, A., Comoglio, P.M., Louvard, D. & Arpin, M. Ezrin is an effector of hepatocyte growth factor-mediated migration and morphogenesis in epithelial cells. *J. Cell Biol.* **138**, 423–434 (1997).
23. Nestl, A., *et al.* Gene expression patterns associated with the metastatic phenotype in rodent and human tumors. *Cancer Res.* **61**, 1569–1577 (2001).
24. Gautreau, A., Louvard, D. & Arpin, M. ERM proteins and NF2 tumor suppressor: the Yin and Yang of cortical actin organization and cell growth signaling. *Curr. Opin. Cell Biol.* **14**, 104–109 (2002).
25. Etienne-Manneville, S. & Hall, A. Rho GTPases in cell biology. *Nature* **420**, 629–635 (2002).
26. Sahai, E. & Marshall, C.J. RHO-GTPases and cancer. *Nat. Rev. Cancer* **2**, 133–142 (2002).
27. Takahashi, K. *et al.* Direct interaction of the Rho GDP dissociation inhibitor with ezrin/radixin/moesin initiates the activation of the Rho small G protein. *J. Biol. Chem.* **272**, 23371–23375 (1997).
28. Lamb, R.F. *et al.* The TSC1 tumour suppressor hamartin regulates cell adhesion through ERM proteins and the GTPase Rho. *Nat. Cell Biol.* **2**, 281–287 (2000).
29. Ren, X.D., Kiosses, W.B. & Schwartz, M.A. Regulation of the small GTP-binding protein Rho by cell adhesion and the cytoskeleton. *EMBO J.* **18**, 578–585 (1999).
30. Danen, E.H., Sonneveld, P., Sonnenberg, A. & Yamada, K.M. Dual stimulation of Ras/mitogen-activated protein kinase and RhoA by cell adhesion to fibronectin supports growth factor-stimulated cell cycle progression. *J. Cell Biol.* **151**, 1413–1422 (2000).
31. Relaix, F. & Buckingham, M. From insect eye to vertebrate muscle: redeployment of a regulatory network. *Genes Dev.* **13**, 1317–1318 (1999).
32. Heanue, T.A. *et al.* Synergistic regulation of vertebrate muscle development by Dach2, Eya2, and Six1, homologs of genes required for *Drosophila* eye formation. *Genes Dev.* **13**, 3231–3243 (1999).
33. Kardon, G., Heanue, T.A. & Tabin, C.J. Pax3 and Dach2 positive regulation in the developing somite. *Dev. Dyn.* **224**, 350–355 (2002).
34. Laclef, C. *et al.* Altered myogenesis in Six1-deficient mice. *Development* **130**, 2239–2252 (2003).
35. Spitz, F. *et al.* Expression of myogenin during embryogenesis is controlled by Six/sine oculis homeoproteins through a conserved MEF3 binding site. *Proc. Natl. Acad. Sci. USA* **95**, 14220–14225 (1998).
36. Schafer, K. & Braun, T. Early specification of limb muscle precursor cells by the homeobox gene *Lbx1h*. *Nat. Genet.* **23**, 213–216 (1999).
37. Brummelkamp, T.R., Bernards, R. & Agami, R. A system for stable expression of short interfering RNAs in mammalian cells. *Science* **296**, 550–553 (2002).
38. Khan, J. *et al.* Expression profiling in cancer using cDNA microarrays. *Electrophoresis* **20**, 223–229 (1999).
39. Chen, Y., Dougherty, E.R. & Bittner, M.L. Ratio-based decisions and the quantitative analysis of cDNA microarray images. *Biomed. Optics* **2**, 364–374 (1997).
40. Chen, Y. *et al.* Ratio statistics of gene expression levels and applications to microarray data analysis. *Bioinformatics* **18**, 1207–1215 (2002).
41. Ringner, M., Peterson, C. & Khan, J. Analyzing array data using supervised methods. *Pharmacogenomics* **3**, 403–415 (2002).
42. Yu, Y. & Merlino, G. Constitutive c-Met signaling through a nonautocrine mechanism promotes metastasis in a transgenic transplantation model. *Cancer Res.* **62**, 2951–2956 (2002).
43. Shao, R. *et al.* Inhibition of nuclear factor- $\kappa$ B activity is involved in E1A-mediated sensitization of radiation-induced apoptosis. *J. Biol. Chem.* **272**, 32739–32742 (1997).
44. Pollack, A.L., Barth, A.I., Altschuler, Y., Nelson, W.J. & Mostov, K.E. Dynamics of  $\beta$ -catenin interactions with APC protein regulate epithelial tubulogenesis. *J. Cell Biol.* **137**, 1651–1662 (1997).
45. Khanna, C. *et al.* An orthotopic model of murine osteosarcoma with clonally related variants differing in pulmonary metastatic potential. *Clin. Exp. Metastasis* **18**, 261–271 (2000).